

GROWTH OF MASSIVE BLACK HOLES DURING RADIATIVELY INEFFICIENT ACCRETION PHASES

XINWU CAO

Shanghai Astronomical Observatory, Chinese Academy of Sciences, 80 Nandan Road, Shanghai, 200030, China; Email: xwcao@shao.ac.cn
accepted by ApJ

ABSTRACT

We derive the black hole mass density as a function of redshift from the hard X-ray AGN luminosity function assuming that massive black holes grow via accreting the circumnuclear gases. The derived black hole mass density matches the measured local black hole mass density at $z = 0$, which requires the average radiative efficiency of AGNs to be $\sim 0.1 - 0.17$. The massive black holes in most faint active galactic nuclei (AGNs) and even normal galaxies are still accreting gases, though their accretion rates are very low. Radiatively inefficient accretion flows (RIAFs) are supposed in these faint sources, which should radiate mostly in the hard X-ray band. We calculate the contribution to the X-ray background from both the bright AGNs and the RIAFs in faint AGNs/normal galaxies. Our calculations show that both the observed intensity and spectral shape of the XRB with an energy peak at ~ 30 keV can be well reproduced without including the emission of Compton-thick AGNs, if the massive black holes in faint AGNs/normal galaxies are spinning rapidly with $a \sim 0.9$ and accreting at rates $\dot{m} \sim 1.0 - 3.0 \times 10^{-4}$. It indicates that less than ~ 5 per cent of local massive black hole mass density was accreted during radiatively inefficient accretion phases, which is obviously only an upper limit, because Compton-thick AGNs have not been considered. If the same number of the Compton-thick AGNs with $\log N_{\text{H}} = 24 - 25$ as those with $\log N_{\text{H}} = 23 - 24$ is considered, the fraction of local black hole mass density accumulated during inefficient accretion phases should be lower than ~ 2 per cent. The constraints of the XRB can provide upper limits on the average accretion rate for inactive galaxies.

Subject headings: galaxies: active—quasars: general—accretion, accretion disks—black hole physics; X-rays: diffuse background

1. INTRODUCTION

There is evidence that most nearby galaxies contain massive black holes at their centers, and a tight correlation was revealed between central massive black hole mass and the velocity dispersion of the galaxy (Ferrarese & Merritt 2000; Gebhardt et al. 2000), which strongly suggests co-evolution of massive black holes and their host galaxies. This correlation, together with the correlation between black hole mass and the host galactic bulge luminosity, are widely used to estimate the black hole masses in galaxies.

The growth of massive black holes may probably be linked to accretion processes (Soltan 1982). Yu & Tremaine (2002) estimated the black hole masses from the stellar velocity dispersions of galaxies measured by the Sloan Digital Sky Survey (SDSS) using the empirical relation between black hole mass and the velocity dispersion, and the local black hole mass density was derived. They further calculated the black hole mass density accreted during optical bright quasar phases using an optical quasar luminosity function (LF), and found that the accreted mass density is consistent with the local black hole mass density estimated from the velocity dispersions, if a radiative efficiency ~ 0.1 is adopted for quasars. This implies that the growth of massive black holes may be dominantly through accretion during optically bright quasar phases. The optical quasar LF is directly linked to the accretion history of massive black holes, however, it has overlooked many faint AGNs and type II AGNs. The X-ray luminosity functions (XLFs) derived from the surveys in the soft X-ray band ($\lesssim 3$ keV) may have missed many obscured (type II) AGNs, while the hard X-ray surveys ($\sim 2-10$ keV) can trace the whole AGN population including obscured type II AGNs and extend to low X-ray luminosity (Ueda et al. 2003), thus providing a useful tool to explore the accretion history of

AGNs in the universe. Many works on XLFs were carried out in either the soft X-ray band ($\lesssim 3$ keV) (e.g., Maccacaro et al. 1991; Boyle et al. 1993; Page et al. 1997; Miyaji et al. 2000) or the hard X-ray band ($\gtrsim 2$ keV) (e.g., Boyle et al. 1998; Cowie et al. 2003; Ueda et al. 2003).

The cosmological X-ray background (XRB) is mostly contributed by AGNs (Hasinger 1998; Schmidt et al. 1998). In the most popular synthesis models of the XRB based on the unification schemes for AGNs, the cosmological XRB from $\lesssim 2$ keV to more than several hundred keV can be fairly well reproduced by using a series of template spectra of AGNs with different obscuration, which are derived by assuming an intrinsic AGN spectrum consisting of a power-law X-ray spectrum with an exponential cutoff around several hundred keV (see, e.g., Matt & Fabian 1994; Madau et al. 1994; Comastri et al. 1995; Gilli et al. 1999; Ueda et al. 2003). Di Matteo & Fabian (1997) have alternatively proposed that the hard XRB above 10 keV may be dominated by the thermal bremsstrahlung emission from the advection dominated accretion flows (ADAFs) in low-luminosity AGNs. Further detailed ADAF spectral calculations (Di Matteo et al. 1999) have shown that many sources at redshift $z \sim 2 - 3$ with ADAFs accreting at the rates close to the critical value would be required to reproduce the observed XRB spectral shape with an energy peak at ~ 30 keV.

Recently, Ueda et al. (2003) derived a hard X-ray luminosity function (HXLF) from a highly complete AGN sample (2-10 keV), which includes both type I and type II AGNs (except Compton-thick AGNs). Based on this HXLF, their synthesis models can explain most of the observed XRB from the soft X-ray band to the hard X-ray band around several hundred keV. Their calculations slightly ($\approx 10-20\%$) underestimate the relative shape of the XRB spectrum around its peak intensity (see Fig. 18 in their work). Such a discrepancy can be ex-

plained provided the same number of Compton-thick AGNs with $\log N_{\text{H}} = 24 - 25$ as those with $\log N_{\text{H}} = 23 - 24$ is included. As the number density of Compton-thick AGNs is still quite uncertain, the residual XRB could be attributed to both the Compton-thick AGNs with $\log N_{\text{H}} = 24 - 25$ and the RIAFs in faint AGNs/normal galaxies. Although their relative importance is still unclear, it is obvious that the spectral shape of the observed XRB cannot be solely attributed to the RIAFs/ADAFs in Seyferts.

There are a variety of studies exploring the evolution of AGNs based on either optical quasar LFs or XLFs, or both (e.g., Haehnelt & Rees 1993; Haiman & Menou 2000; Kauffmann & Haehnelt 2000; Yu & Tremaine 2002; Wyithe & Loeb 2003; Marconi et al. 2004; Hopkins et al. 2005). A common conclusion is that the timescale of AGN activities is short compared with the Hubble timescale, though the quantitative results on the bright quasar lifetime vary from $\sim 10^7$ to $\sim 10^9$ years for different investigations. The standard optically thick accretion disks are present in bright AGNs, as their accretion rates are high. The AGN activity may be switched off while the gases near the black hole are exhausted (see Narayan 2002, for a review, and the references therein). When the accretion rate \dot{m} ($\dot{m} = \dot{M}/\dot{M}_{\text{Edd}}$) declines below a critical value $\dot{m}_{\text{crit}} \sim 0.01$, the standard disk transits to a RIAF (e.g., Narayan & Yi 1995). RIAFs are optically thin, very hot, and their spectra are peaked in the hard X-ray band. In a previous work, Cao (2005) calculated the contribution to the hard XRB from the RIAFs in the faint AGNs. It was found that the accretion rate \dot{m} must decrease rapidly to far below the critical rate \dot{m}_{crit} after the accretion mode transition, otherwise, the RIAFs may produce too much hard X-ray emission to match the observed hard XRB. This implies that the growth of massive black holes during radiatively inefficient accretion phases is not important. Hopkins et al. (2006) considered the distribution of local supermassive black hole Eddington ratios and accretion rates, and they found that black hole mass growth, both of the integrated mass density and the masses of most individual objects, are dominated by an earlier, radiatively efficient, high accretion rate stage, and not by the radiatively inefficient low accretion rate phases.

In this paper, we will explore quantitatively on how much mass in the local massive black holes was accreted during their radiatively inefficient accretion phases from the constraint of the XRB. The cosmological parameters $\Omega_{\text{M}} = 0.3$, $\Omega_{\Lambda} = 0.7$, and $H_0 = 70 \text{ km s}^{-1} \text{ Mpc}^{-1}$ have been adopted in this work.

2. BLACK HOLE MASS DENSITY

The HXLF given by Ueda et al. (2003) is so far most suitable for our present investigation, as it includes both type I and type II AGNs (except Compton-thick AGNs). The HXLF in 2–10 keV derived by Ueda et al. (2003) is

$$\frac{d\Phi(L_X, z)}{d\text{Log}L_X} = \frac{d\Phi(L_X, 0)}{d\text{Log}L_X} e(z, L_X), \quad (1)$$

where

$$\frac{d\Phi(L_X, z=0)}{d\text{Log}L_X} = A[(L_X/L_*)^{\gamma_1} + (L_X/L_*)^{\gamma_2}]^{-1}, \quad (2)$$

$$e(z, L_X) = \begin{cases} (1+z)^{p1} & (z < z_c(L_X)) \\ e(z_c)[(1+z)/(1+z_c(L_X))]^{p2} & (z \geq z_c(L_X)), \end{cases} \quad (3)$$

and

$$z_c(L_X) = \begin{cases} z_c^* & (L_X \geq L_a) \\ z_c^*(L_X/L_a)^\alpha & (L_X < L_a). \end{cases} \quad (4)$$

All the parameters for our present adopted cosmology are as follows: $A = 5.04(\pm 0.33) \times 10^{-6} \text{ Mpc}^{-3}$, $\log L_* (\text{ergs s}^{-1}) = 43.94_{-0.26}^{+0.21}$, $\gamma_1 = 0.86 \pm 0.15$, $\gamma_2 = 2.23 \pm 0.13$, $p1 = 4.23 \pm 0.39$; $p2 = -1.5$, $z_c = 1.9$, and $\log L_a (\text{ergs s}^{-1}) = 44.6$ (Ueda et al. 2003). All the sources described by Ueda et al. (2003)'s HXLF have hard X-ray luminosities $L_X^{2-10 \text{ keV}}$ between $10^{41.5} - 10^{48} \text{ ergs s}^{-1}$. In this work, we refer to the sources described by the Ueda et al. (2003)'s HXLF as active galaxies, while all the remainder with $L_X^{2-10 \text{ keV}} < 10^{41.5} \text{ ergs s}^{-1}$ as inactive galaxies.

The cosmological evolution of black hole mass density caused by accretion during active galaxy phases is described by

$$\frac{d\rho_{\text{bh}}^{\text{A}}(z)}{dz} = \frac{dt}{dz} \frac{1}{M_{\odot}} \int_{41.5}^{48} \frac{(1-\epsilon)f_{\text{cor}}L_X}{\epsilon c^2} \frac{d\Phi(L_X, z)}{d\text{Log}L_X} d\text{Log}L_X, \quad (5)$$

where $\Phi(L_X, z)$ is the HXLF given by Eq. (1), $\rho_{\text{bh}}^{\text{A}}(z)$ (in units of $M_{\odot} \text{ Mpc}^{-3}$) is the black hole mass density accreted during active galaxy phases between z and z_{max} , and ϵ is the radiative efficiency for AGNs. The ratio f_{cor} of the bolometric luminosity to the X-ray luminosity in 2–10 keV is given by

$$\log f_{\text{cor}} = 1.54 + 0.24\mathcal{L} + 0.012\mathcal{L}^2 - 0.0015\mathcal{L}^3, \quad (6)$$

where $\mathcal{L} = \log L_{\text{bol}}/L_{\odot} - 12$, and L_{bol} is the bolometric luminosity (Marconi et al. 2004).

The central massive black holes in inactive galaxies may still be accreting gases, though the accretion rates may be very low as their hard X-ray luminosities $L_X^{2-10 \text{ keV}}$ are below $10^{41.5} \text{ ergs s}^{-1}$. The Eddington accretion rate $\dot{M}_{\text{Edd}} = (M_{\text{bh}}/M_{\odot})L_{\odot, \text{Edd}}/\eta_{\text{eff}}c^2$, where $L_{\odot, \text{Edd}} = 1.38 \times 10^{38} \text{ ergs s}^{-1}$, and a conventional radiative efficiency $\eta_{\text{eff}} = 0.1$ is adopted here. This radiative efficiency η_{eff} is only for the definition of the Eddington rate \dot{M}_{Edd} , and it can be different from the real radiative efficiency ϵ in Eq. (5). When the mass accretion rate \dot{m} ($\dot{m} = \dot{M}/\dot{M}_{\text{Edd}}$) is below a critical value \dot{m}_{crit} , the standard disk converts to a RIAF (e.g., Narayan & Yi 1995). RIAFs should be present in most, if not all, of those inactive galaxies. Besides the black hole mass density $\rho_{\text{bh}}^{\text{A}}(z)$ accreted in active galaxies, we need to calculate the black hole density $\rho_{\text{bh}}^{\text{B}}(z)$ accreted in inactive galaxies. Assuming an average dimensionless mass accretion rate $\dot{m}_{\text{inact}}^{\text{aver}}$ for those inactive galaxies, we can calculate the black hole mass density $\rho_{\text{bh}}^{\text{B}}(z)$ accreted during inactive galaxy phases between z and z_{max} by

$$\frac{d\rho_{\text{bh}}^{\text{B}}(z)}{dz} = \frac{\rho_{\text{bh}}^{\text{inact}}(z)\dot{m}_{\text{inact}}^{\text{aver}}L_{\odot, \text{Edd}}(1-\epsilon^{\text{RIAF}})}{M_{\odot}\eta_{\text{eff}}c^2} \frac{dt}{dz}, \quad (7)$$

where ϵ^{RIAF} is the radiative efficiency of the RIAFs in inactive galaxies, provided the black hole mass density of inactive galaxies $\rho_{\text{bh}}^{\text{inact}}(z)$ (in units of $M_{\odot} \text{ Mpc}^{-3}$) as a function of redshift z is known. Here, $\rho_{\text{bh}}^{\text{inact}}(z)$ is the black hole mass density of inactive galaxies at z , while $\rho_{\text{bh}}^{\text{B}}(z)$ describes the mass density accreted during inactive galaxy phases between z and z_{max} . The radiative efficiency ϵ^{RIAF} is usually much lower than that for standard thin disks. Our numerical calculations for RIAF spectra show that ϵ^{RIAF} is significantly lower than 0.01,

so we approximate $\epsilon^{\text{RIAF}} \simeq 0$ in Eq. (7) while calculating the black hole mass density.

The total black hole mass density $\rho_{\text{bh}}^{\text{acc}}(z)$ accumulated through accretion both in active and inactive galaxies is:

$$\rho_{\text{bh}}^{\text{acc}}(z) = \rho_{\text{bh}}^{\text{A}}(z) + \rho_{\text{bh}}^{\text{B}}(z), \quad (8)$$

i.e., a sum of black hole mass densities accreted in active and inactive galaxy phases. In order to calculate $\rho_{\text{bh}}^{\text{acc}}(z)$, we need to know the black hole mass density of inactive galaxies $\rho_{\text{bh}}^{\text{inact}}(z)$ as a function of z (see Eq. 7). Assuming the growth of massive black holes is dominated by accretion (e.g., Yu & Tremaine 2002), the total black hole mass density is given by

$$\rho_{\text{bh}}(z) \simeq \rho_{\text{bh}}^{\text{acc}}(z) + \rho_{\text{bh}}(z_{\text{max}}) = \rho_{\text{bh}}^{\text{A}}(z) + \rho_{\text{bh}}^{\text{B}}(z) + \rho_{\text{bh}}(z_{\text{max}}), \quad (9)$$

where $\rho_{\text{bh}}(z_{\text{max}})$ is the total black hole mass density at z_{max} . The black hole mass density for active galaxies in the co-moving space at redshift z can be calculated from the XLF by

$$\rho_{\text{bh}}^{\text{act}}(z) = \frac{1}{(\epsilon/\eta_{\text{eff}})\dot{m}_{\text{act}}^{\text{aver}}L_{\text{Edd},\odot}} \int_{41.5}^{48} f_{\text{cor}L_X} \frac{d\Phi(L_X, z)}{d\text{Log}L_X} d\text{Log}L_X \text{ M}_{\odot} \text{Mpc}^{-3}, \quad (10)$$

where $\Phi(L_X, z)$ is the HXLF given by Eq. (1), $\dot{m}_{\text{act}}^{\text{aver}}$ is the average dimensionless accretion rate for the active galaxies. The black hole mass density for inactive galaxies $\rho_{\text{bh}}^{\text{inact}}(z)$ can be derived by subtracting that for active galaxies $\rho_{\text{bh}}^{\text{act}}(z)$ from the total black hole density $\rho_{\text{bh}}(z)$. The black hole mass density of inactive galaxies $\rho_{\text{bh}}^{\text{inact}}(z)$ can therefore be calculated by

$$\rho_{\text{bh}}^{\text{inact}}(z) = \rho_{\text{bh}}(z) - \rho_{\text{bh}}^{\text{act}}(z) = \rho_{\text{bh}}^{\text{A}}(z) + \rho_{\text{bh}}^{\text{B}}(z) + \rho_{\text{bh}}(z_{\text{max}}) - \rho_{\text{bh}}^{\text{act}}(z). \quad (11)$$

Assuming all galaxies are active at $z = z_{\text{max}}$ (e.g., Marconi et al. 2004), the black hole mass density $\rho_{\text{bh}}(z_{\text{max}}) = \rho_{\text{bh}}^{\text{act}}(z_{\text{max}})$ is available by using Eq. (10). At $z = z_{\text{max}}$, $\rho_{\text{bh}}^{\text{A}} = \rho_{\text{bh}}^{\text{B}} = 0$. Thus, we integrate Eqs. (5) and (7) simultaneously over z from z_{max} using Eqs. (10) and (11), and the black hole mass densities as functions of z are finally available provided the three parameters: $\dot{m}_{\text{act}}^{\text{aver}}$, $\dot{m}_{\text{inact}}^{\text{aver}}$ and ϵ are specified. We adopt $z_{\text{max}} = 5$ and $\dot{m}_{\text{act}}^{\text{aver}} = 0.1$ in all our calculations. The value of the radiative efficiency ϵ is tuned to let the derived total black hole mass density $\rho_{\text{bh}}(z)$ match $\rho_{\text{bh}}^{\text{local}}$ at $z = 0$, for a given $\dot{m}_{\text{inact}}^{\text{aver}}$.

The local black hole mass density $\rho_{\text{bh}}^{\text{local}}$ was estimated from the stellar velocity dispersion measured with the SDSS by using the relation between black hole mass and the stellar velocity dispersion. The resulting local black hole mass densities vary from $\sim 2 \times 10^5$ to $5 \times 10^5 \text{M}_{\odot} \text{Mpc}^{-3}$ (e.g., Salucci et al. 1999; Yu & Tremaine 2002; Sheth et al. 2003; Marconi et al. 2004). In some previous works, the black hole mass densities as functions of redshift were derived to match the measured local black hole mass density by integrating AGN LFs (e.g., Yu & Tremaine 2002; Marconi et al. 2004). The difference between these previous works and ours is that we have included the contribution to the local black hole mass density from accretion in inactive galaxies.

Our calculations are carried out for two different values of the local black hole mass density: $\rho_{\text{bh}}^{\text{local}} = 2.5 \times 10^5 \text{M}_{\odot} \text{Mpc}^{-3}$, and $4.0 \times 10^5 \text{M}_{\odot} \text{Mpc}^{-3}$, respectively, considering the different values of $\rho_{\text{bh}}^{\text{local}}$ derived in the literature (e.g., Salucci et al. 1999; Yu & Tremaine 2002; Sheth et al.

2003; Marconi et al. 2004). We find that the radiative efficiencies $\epsilon \sim 0.07 - 0.12$ are required, so that the total black hole mass densities accumulated through accretion can match the measured local black hole mass densities (see Figs. 1, and Table 1 for a summary of the results). The derived radiative efficiency depends only weakly on $\dot{m}_{\text{inact}}^{\text{aver}}$, because most of black hole mass was accreted during active galaxy phases. If the average mass accretion rate $\dot{m}_{\text{inact}}^{\text{aver}}$ is high, a significant fraction of local black hole mass density was accumulated in inactive galaxies (~ 16 per cent, for $\dot{m}_{\text{inact}}^{\text{aver}} = 0.001$, see Table 1). If $\dot{m}_{\text{inact}}^{\text{aver}} \lesssim 3 \times 10^{-4}$, less than ~ 5 per cent of local black hole mass density was accreted in inactive galaxies. At low redshifts with $z \lesssim 2$, the black hole mass density is dominated by the black holes in inactive galaxies (see Fig. 2). In Fig. 2, we find that the derived black hole mass densities $\rho_{\text{bh}}^{\text{inact}}(z)$ in inactive galaxies at low redshifts mainly depend on the value of the measured local black hole mass density $\rho_{\text{bh}}^{\text{local}}$ adopted.

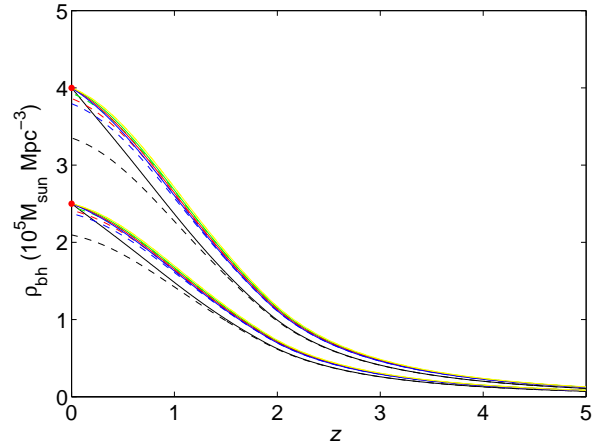


FIG. 1.— The total black hole mass densities $\rho_{\text{bh}}(z)$ accumulated through accretion as functions of redshift z (solid lines), while the black hole mass densities accreted during active galaxy phases only [$\rho_{\text{bh}}^{\text{A}}(z) + \rho_{\text{bh}}(z_{\text{max}})$] are plotted as dashed lines. The upper set of curves is derived for $\rho_{\text{bh}}^{\text{local}} = 4.0 \times 10^5 \text{M}_{\odot} \text{Mpc}^{-3}$, while the lower one is for $\rho_{\text{bh}}^{\text{local}} = 2.5 \times 10^5 \text{M}_{\odot} \text{Mpc}^{-3}$. The different colors correspond to different models: black (Model A), blue (Model B), red (Model C), green (Model D), and yellow (Model E). The description of different models is summarized in Table 1.

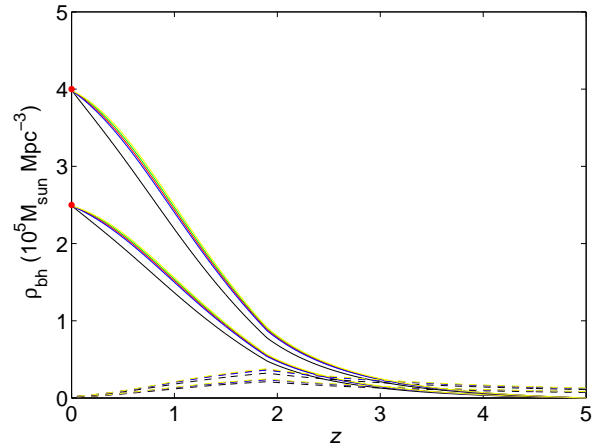


FIG. 2.— The black hole mass densities $\rho_{\text{bh}}^{\text{inact}}(z)$ for inactive galaxies as functions of redshift z (solid lines), while the dashed lines represent the black hole mass densities $\rho_{\text{bh}}^{\text{act}}(z)$ in active galaxies. The upper set of curves is derived for $\rho_{\text{bh}}^{\text{local}} = 4.0 \times 10^5 \text{M}_{\odot} \text{Mpc}^{-3}$, while the lower one is for $\rho_{\text{bh}}^{\text{local}} = 2.5 \times 10^5 \text{M}_{\odot} \text{Mpc}^{-3}$. The different colors correspond to different models: black (Model A), blue (Model B), red (Model C), green (Model D), and yellow (Model E). The description of different models is summarized in Table 1.

3. RIAF SPECTRA

The RIAF spectrum is almost proportional to black hole mass M_{bh} for a given dimensionless mass accretion rate \dot{m} . In order to calculate the contribution of the RIAFs in all inactive galaxies to the XRB, we need to use the X-ray spectrum $l_{\text{X}}(E)$ of a RIAF around a 10^8M_{\odot} black hole accreting at the rate $\dot{m}_{\text{inact}}^{\text{aver}}$ as a template spectrum. We employ the approach suggested by Manmoto (2000) to calculate the global structure of an accretion flow surrounding a massive black hole in the general relativistic frame, which allows us to calculate the structure of an accretion flow surrounding either a spinning or non-spinning black hole. All the radiation processes are included in the calculations of the global accretion flow structure (see Manmoto 2000, for details and the references therein). However, the values of some parameters adopted are different from those in Manmoto (2000) (see discussion in §5, and Cao 2005). In the spectral calculations, the gravitational redshift effect is considered, while the relativistic optics near the black hole is neglected. This will not affect our final results on the XRB, as the inactive galaxies should have randomly distributed orientations and the stacked spectra would not be affected by the relativistic optics.

The global structure of a RIAF surrounding a black hole spinning at a with mass M_{bh} can be calculated, if some parameters, \dot{m} , α , β and δ , are specified. The parameter δ describes the fraction of the viscously dissipated energy directly going into electrons in the accretion flow. The three-dimensional MHD simulations suggest that the viscosity parameter α in the accretion flows is ~ 0.1 (Armitage 1998), or $\sim 0.05 - 0.2$ (Hawley & Balbus 2002). The critical accretion rate $\dot{m}_{\text{crit}} \simeq 0.01$ is suggested by different authors either from observations or theoretical arguments (see Narayan 2002, for a review, and the references therein). Our numerical calculations for the global structure of the flows show $\dot{m}_{\text{crit}} \simeq 0.01$ for $\alpha = 0.2$. Thus, we adopt $\alpha = 0.2$ in this work. The parameter β , defined as $p_{\text{m}} = B^2/8\pi = (1 - \beta)p_{\text{tot}}$ ($p_{\text{tot}} = p_{\text{gas}} + p_{\text{m}}$), describes the magnetic field strength of the accretion flow. This parameter is in fact not a free parameter, which is related to the viscosity parameter α as $\beta \simeq (6\alpha - 3)/(4\alpha - 3)$, as suggested by the MHD simulations (Hawley, Gammie & Balbus 1996; Narayan, Mahadevan & Quataert 1998). For $\alpha = 0.2$, $\beta \simeq 0.8$ is required. It was pointed out that a significant fraction of the viscously dissipated energy could go into electrons by magnetic reconnection, if the magnetic fields in the flow are strong (Bisnovatyi-Kogan & Lovelace 1997, 2000). In our calculations, we adopt a conventional value of $\delta = 0.1$ in all the calculations. We plot the X-ray spectra of the RIAFs accreting at different rates for Schwarzschild holes in Fig. 3. The spectra of the accretion flows surrounding the Kerr black holes with $a = 0.9$ are plotted in Fig. 4.

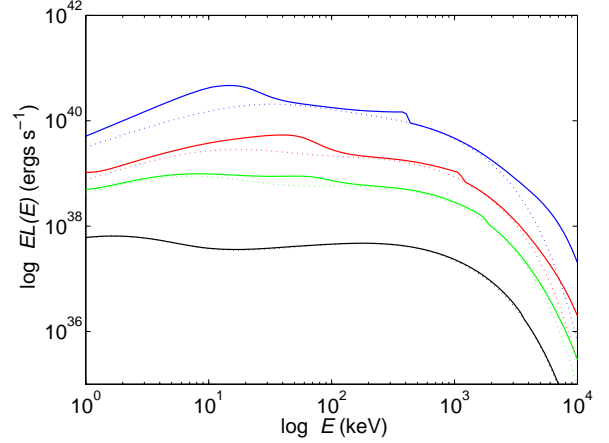


FIG. 3.— The spectra of the RIAFs surrounding Schwarzschild black holes with 10^8M_{\odot} accreting at different rates: $\dot{m} = 1.0 \times 10^{-3}$ (blue lines), 5.0×10^{-4} (red lines), 3.0×10^{-4} (green lines), and 1.0×10^{-4} (black lines). The viscosity parameter $\alpha = 0.2$, the fraction of the magnetic pressure $1 - \beta = 0.2$, and the fraction of viscously dissipated energy directly heating the electrons $\delta = 0.1$, are adopted in the calculations. The solid lines represent the spectra of the RIAFs, while the dotted lines represent their bremsstrahlung spectra only.

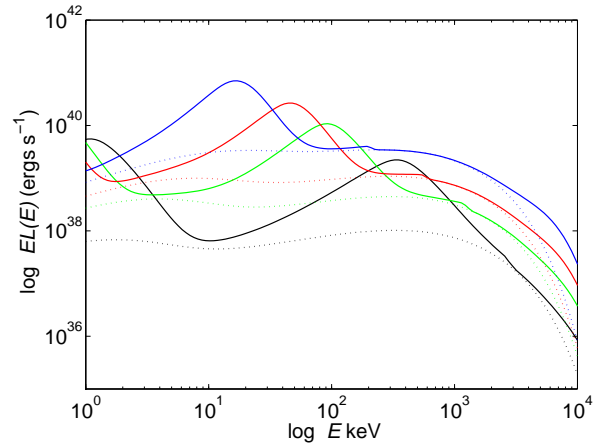


FIG. 4.— The spectra of the RIAFs surrounding Kerr black holes ($a = 0.9$) with 10^8M_{\odot} accreting at different rates: $\dot{m} = 5.0 \times 10^{-4}$ (blue lines), 3.0×10^{-4} (red lines), 2.0×10^{-4} (green lines), and 1.0×10^{-4} (black lines). The same disk parameters are adopted in the calculations as those in Fig. 3. The solid lines represent the spectra of the RIAFs, while the dotted lines represent their bremsstrahlung spectra only.

4. CONTRIBUTION TO THE XRB FROM THE RIAFs IN INACTIVE GALAXIES

The contribution of the RIAFs in all inactive galaxies to the cosmological XRB can be calculated by

$$f_{\text{X}}(E) = \frac{1}{10^8 \text{M}_{\odot}} \int_0^{z_{\text{max}}} \frac{\rho_{\text{bh}}^{\text{inact}}(z)(1+z)l_{\text{X}}[(1+z)E] dV}{4\pi d_L^2} dz, \quad (12)$$

where $l_{\text{X}}(E)$ is the spectrum of a RIAF surrounding a 10^8M_{\odot} black hole accreting at $\dot{m}_{\text{inact}}^{\text{aver}}$, which is calculated as described in §3.

There is no doubt that the contribution from active galaxies is important to the XRB, as the *BeppoSAX* observations showed that the power-law X-ray spectra of bright AGNs extends to several hundred keV (e.g., Nicastro et al. 2000).

Ueda et al. (2003) adopted a template intrinsic AGN spectrum, i.e., a power law+an exponential spectrum with cutoff energy E_c of 500 keV, in their XRB synthesis model calculations. They also included the contribution to the XRB by the Compton-thick AGNs with $\log N_H = 24-25$ assuming a fixed ratio to those with $\log N_H = 23-24$ without considering the redshift dependence of the ratio. The effects of Compton scattering leading to significant decrease of the emitted flux of the nucleus even in the hard X-ray bands have been properly considered in their calculations, while the contribution of the sources with $\log N_H > 25$ is neglected by assuming that all X-rays are absorbed. In this work, we simply adopt the results of their XRB synthesis model calculations for AGNs. We consider that the XRB consists not only of the emission from type I/II bright AGNs (Compton-thin) described by the HXLF, but also of the emission from RIAFs in those inactive galaxies that are not included in this HXLF. All curves of the XRB synthesis for Compton thin/thick AGNs plotted in the figures of this work are taken from Ueda et al. (2003). In Figs. 5 and 6, we plot the XRBs contributed by both active galaxies and inactive galaxies with different parameters adopted, and compare them with the observed XRB. Here, the contribution from Compton-thick AGNs has not been included, which may be unrealistic, because Compton-thick AGNs have already been detected, though their number density is still quite uncertain. However, these calculations, at least, provide strict constraints (upper limits) on the average mass accretion rates of inactive galaxies. We define a parameter ξ to describe the number ratio of Compton-thick AGNs with $\log N_H = 24-25$ to those with $\log N_H = 23-24$. In Fig. 7, we plot the results of the XRB synthesis, in which the contribution of Compton-thick AGNs is considered by assuming $\xi = 0.5$ and 1.0, respectively. For a given ξ , the average accretion rate $\dot{m}_{\text{inact}}^{\text{aver}}$ is tuned in order not to overproduce the observed XRB in 10-30 keV (Ueda et al. 2003). Thus, the constraints (upper limits) on the average accretion rates $\dot{m}_{\text{inact}}^{\text{aver}}$ for inactive galaxies from the cosmological XRB are plotted as functions of ξ in Fig. 8.

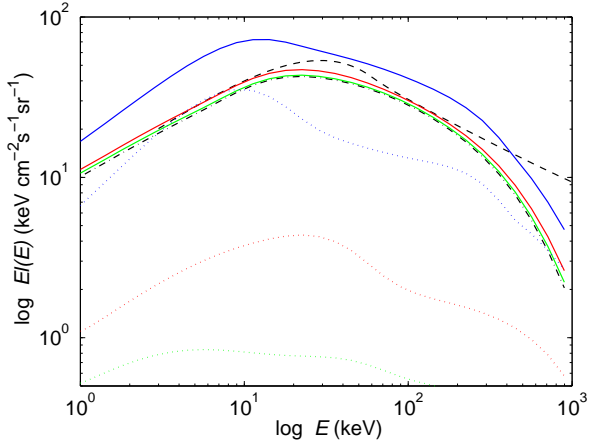


FIG. 5.— The contribution to the XRB from active galaxies and the RIAFs surrounding Schwarzschild black holes in inactive galaxies. The dashed line is the observed XRB (taken from Ueda et al. 2003). The dot-dashed line represents the contribution by type I/II AGNs (Compton-thin), which is taken from Ueda et al. (2003). The lines with different colors represent the XRB synthesis model calculations for different values of the average accretion rates for inactive galaxies: $\dot{m}_{\text{inact}}^{\text{aver}} = 1.0 \times 10^{-3}$ (blue), 5.0×10^{-4} (red), and 3.0×10^{-4} (green). The solid lines represent the XRB contributed by type I/II (Compton-thin) active galaxies described by the HXLF and the RIAFs in all inactive galaxies, while the dotted lines are only for the contributions from the RIAFs in all inactive galaxies. The black hole mass density for inactive galaxies $\rho_{\text{bh}}^{\text{inact}}(z)$ used in the XRB synthesis calculations is derived for $\rho_{\text{bh}}^{\text{local}} = 4.0 \times 10^5 M_{\odot} \text{Mpc}^{-3}$.

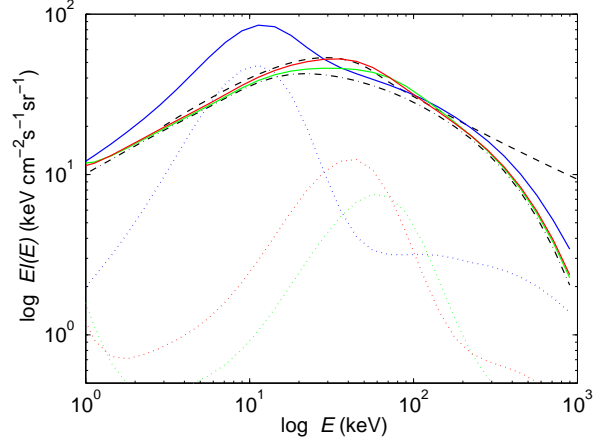


FIG. 6.— The same as Fig. 5, but for the RIAFs surrounding the Kerr black holes with $a = 0.9$ in inactive galaxies. The lines with different colors represent different values of the average accretion rates: $\dot{m}_{\text{inact}}^{\text{aver}} = 5.0 \times 10^{-4}$ (blue), 2.5×10^{-4} (red), and 2.0×10^{-4} (green).

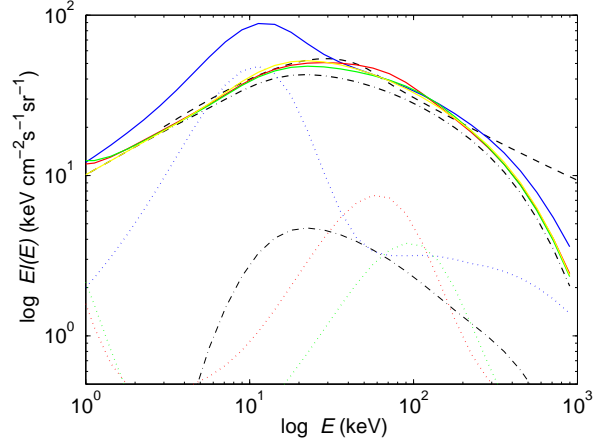


FIG. 7.— The same as Fig. 5, but for the Kerr black holes with $a = 0.9$ and the contribution of Compton-thick AGNs is included. The thin dash-dotted line represents the contribution of Compton-thick AGNs (taken from Ueda et al. 2003). The yellow line represents the synthesis model for type I/II+Compton-thick AGNs assuming $\xi = 1.0$, in which the contribution from the RIAFs in inactive galaxies is not included (taken from Ueda et al. 2003). All lines with other colors correspond to the XRB synthesis model calculations by assuming $\xi = 0.5$, i.e., the number of Compton-thick AGNs with $\log N_H = 24-25$ is half of those with $\log N_H = 23-24$. These lines represent different values of the average accretion rates: $\dot{m}_{\text{inact}}^{\text{aver}} = 5.0 \times 10^{-4}$ (blue), 2.0×10^{-4} (red), and 1.5×10^{-4} (green). The local black hole mass density $\rho_{\text{bh}}^{\text{local}} = 4.0 \times 10^5 M_{\odot} \text{Mpc}^{-3}$ is adopted to derive the black hole mass density $\rho_{\text{bh}}^{\text{inact}}(z)$ in inactive galaxies.

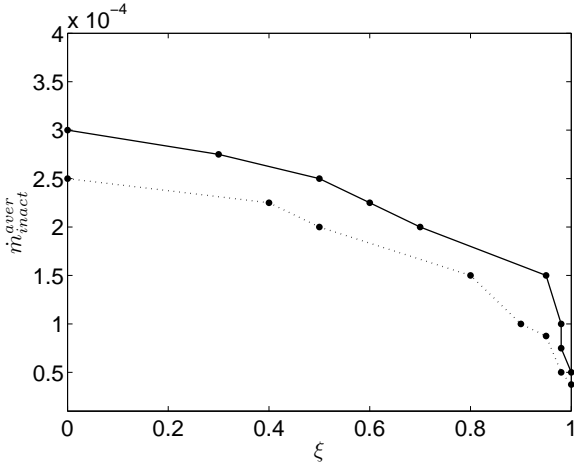


FIG. 8.— The constraints (upper limits) on the average mass accretion rates $\dot{m}_{\text{inact}}^{\text{aver}}$ as functions of the number ratio ξ of the Compton-thick AGNs with $\log N_{\text{H}} = 24-25$ to those with $\log N_{\text{H}} = 23-24$. The solid line represents the result for $\rho_{\text{bh}}^{\text{local}} = 2.5 \times 10^5 M_{\odot} \text{Mpc}^{-3}$, while the dotted line is for $\rho_{\text{bh}}^{\text{local}} = 4.0 \times 10^5 M_{\odot} \text{Mpc}^{-3}$.

5. DISCUSSION

As described in §2, we derive the black hole mass densities for active/inactive galaxies as functions of redshift from the HXLF assuming that massive black holes grow through accretion. Using different measurements on the local black hole mass density, the radiative efficiencies ϵ derived are required to be in the range of $\sim 0.07-0.12$ ($\epsilon \sim 0.11-0.12$, for $\rho_{\text{bh}}^{\text{local}} = 2.5 \times 10^5 M_{\odot} \text{Mpc}^{-3}$, and $\epsilon \sim 0.07-0.08$, for $\rho_{\text{bh}}^{\text{local}} = 4.0 \times 10^5 M_{\odot} \text{Mpc}^{-3}$, see Table 1 for detailed results). If part of the local black hole mass density is accumulated through the way other than accretion, the derived radiative efficiencies should be even higher than the present values. If $\dot{m}_{\text{inact}}^{\text{aver}} \lesssim 3 \times 10^{-4}$, less than ~ 5 per cent of local black hole mass density was accreted in inactive galaxies.

The black hole mass density $\rho_{\text{bh}}^{\text{inact}}(z)$ for inactive galaxies is derived in this work without considering Compton-thick AGNs. The total black hole mass density $\rho_{\text{bh}}(z)$ derived in this work has been affected little by Compton-thick AGNs at low redshifts, because it is derived to match the local black hole mass density at $z=0$. Our calculations may underestimate the black hole mass density $\rho_{\text{bh}}^{\text{act}}(z)$ in active galaxies. Thus, the derived black hole mass density $\rho_{\text{bh}}^{\text{inact}}(z)$ for inactive galaxies should be overestimated (see Eq. 11). Fortunately, the derived $\rho_{\text{bh}}^{\text{inact}}(z)$ has been affected very little at low redshifts, because only a small fraction of massive black holes are active at $z \lesssim 1$ (see Fig. 2). The contribution to the XRB from inactive galaxies is dominated by that from the sources at low redshifts, which means that our main conclusions drawn from the XRB synthesis calculations will not be altered, even if Compton-thick AGNs are included in black hole mass density calculations.

The derived radiative efficiencies ϵ would be higher than the present values listed in Table 1, if Compton-thick AGNs are included. If the ratio of Compton-thick to Compton-thin AGNs is x , a rough estimate gives the radiative efficiencies should be $1+x$ times of the present values, because only about $1/(1+x)$ of the local black hole mass density was accumulated in Compton-thin AGNs and inactive galaxies. Thus, the present derived radiative efficiencies ϵ are only the lower limits. If $x = 0.6$ is adopted (e.g., Tamura et al. 2006), the

radiative efficiencies are about 1.6 times of the present values, i.e., $\epsilon \sim 0.17$ for $\rho_{\text{bh}}^{\text{local}} = 2.5 \times 10^5 M_{\odot} \text{Mpc}^{-3}$, or ~ 0.11 for $\rho_{\text{bh}}^{\text{local}} = 4.0 \times 10^5 M_{\odot} \text{Mpc}^{-3}$, which implies that most massive black holes are spinning rapidly. Elvis et al. (2002) suggested that a high average radiative efficiency $\epsilon \gtrsim 0.15$ is required from the XRB, and they concluded that most massive black holes must be spinning rapidly. Recently, Wang et al. (2006) have estimated the average radiative efficiencies of a large sample of quasars selected from the Sloan Digital Sky Survey (SDSS), by combining their luminosity function and their black hole mass function, and found that quasars have average radiative efficiencies of 0.3–0.35, which implies that the black holes are spinning very rapidly. Our present results seem to be consistent with those derived by Elvis et al. (2002), if suitable number of Compton-thick AGNs is considered.

McLure & Dunlop (2004) estimated that the average accretion rate $\dot{m}_{\text{act}}^{\text{aver}}$ varies from 0.1 at $z \sim 0.2$ to 0.4 at $z \sim 2$ from a large sample of SDSS quasars. The average accretion rate $\dot{m}_{\text{act}}^{\text{aver}} = 0.1$ is adopted in this work to estimate the inactive galaxy black hole mass density $\rho_{\text{bh}}^{\text{inact}}(z)$. We find that the value of $\dot{m}_{\text{act}}^{\text{aver}}$ may affect the resulting $\rho_{\text{bh}}^{\text{inact}}(z)$ very slightly at low redshifts, because $\rho_{\text{bh}}^{\text{inact}}(z) \gg \rho_{\text{bh}}^{\text{act}}(z)$ except at high redshifts ($z \gtrsim 2$, see Fig. 2). The derived black hole mass density $\rho_{\text{bh}}^{\text{inact}}(z)$ for inactive galaxies is mostly governed by the value of local black hole mass density $\rho_{\text{bh}}^{\text{local}}$ at low redshifts. The XRB is mainly contributed by the sources at low redshifts, which implies that the value $\dot{m}_{\text{act}}^{\text{aver}}$ only affect our calculations of the XRB very little.

A small fraction of the sources described by the HXLF with very high hard X-ray luminosities $\sim 10^{47-48} \text{ ergs s}^{-1}$ are probably blazars (e.g., Ueda et al. 2003). For those blazars, the beamed X-ray emission from their jets may dominate over that from the accretion disks, which may lead to over-estimate of the black hole mass density accumulated through accretion. We perform the calculations of the black hole mass densities only for the sources with hard X-ray luminosities in the range of $10^{41.5} - 10^{46} \text{ ergs s}^{-1}$, and find that the fraction of total black hole mass density contributed by these X-ray luminous sources with $L_{\text{X}}^{2-10 \text{ keV}} \geq 10^{46} \text{ ergs s}^{-1}$ can be neglected ($\lesssim 1\%$).

We calculate the spectra of the RIAFs surrounding Schwarzschild black holes ($a=0$), and the Kerr black holes with $a=0.9$ using reasonable parameters for the RIAFs (see discussion in §3), respectively. For the RIAFs surrounding Schwarzschild black holes, we find that the X-ray spectra are dominated by the bremsstrahlung emission if the accretion rates are low (see Fig. 3), while the Comptonization is important for the RIAFs surrounding Kerr black holes (see Fig. 4). For a Kerr black hole, the accretion flow extends to a smaller radius and the gas density is higher at its inner edge compared with that for a Schwarzschild black hole, if they are accreting at the same rate. Thus, the Comptonization becomes significant for the RIAFs surrounding the Kerr black holes. Our calculations show that the peak energy of the spectrum decreases with increasing the accretion rate $\dot{m}_{\text{inact}}^{\text{aver}}$. For the accretion flow with a higher $\dot{m}_{\text{inact}}^{\text{aver}}$, the density at its inner edge is also higher that leads to a lower turnover frequency for the synchrotron radiation from the accretion flow, and then leads to a lower energy peak produced by the Comptonization, because the electron temperatures of the accretion flows at their inner edges are roughly similar for different values of $\dot{m}_{\text{inact}}^{\text{aver}}$.

To compare our calculations of the XRB contributed by ac-

time/inactive galaxies with the observed XRB, we find that the average accretion rate of inactive galaxies $\dot{m}_{\text{inact}}^{\text{aver}}$ should be less than 0.001, otherwise, the calculated XRB will surpass the observed XRB. Our calculations show that $\dot{m}_{\text{inact}}^{\text{aver}} \lesssim 2-3 \times 10^{-4}$ is required by the observed XRB (see Figs. 5 and 6). It is interesting to find that the spectral shape of the observed XRB (peaked at ~ 30 keV) cannot be well fitted by using any value of $\dot{m}_{\text{inact}}^{\text{aver}}$ for Schwarzschild black holes, while both the observed intensity and the spectral shape of the XRB can be well reproduced if $\dot{m}_{\text{inact}}^{\text{aver}} \simeq 2.5 \times 10^{-4}$ is adopted for the Kerr black holes with $a = 0.9$ (see Fig. 6 for $\rho_{\text{bh}}^{\text{local}} = 4.0 \times 10^5 M_{\odot} \text{Mpc}^{-3}$). This implies that most massive black holes are spinning rapidly, which seems to be consistent with the relatively high average radiative efficiencies derived from the XLF (see discussion in the second paragraph of this section). A slightly higher average accretion rate $\dot{m}_{\text{inact}}^{\text{aver}} \simeq 3.0 \times 10^{-4}$ is required for the case of $\rho_{\text{bh}}^{\text{local}} = 2.5 \times 10^5 M_{\odot} \text{Mpc}^{-3}$. Note that the best-fitted value $\dot{m}_{\text{inact}}^{\text{aver}}$ does not depend linearly on $1/\rho_{\text{bh}}^{\text{local}}$, because the luminosity has a non-linear dependence of accretion rate for RIAFs (e.g., Wu & Cao 2006). Here, we have neglected the contribution of the Compton-thick AGNs, as it is still unclear how many Compton-thick AGNs are in the universe (e.g., Ueda et al. 2003). Thus, these results should be only regarded as the upper limits on accretion rates in inactive galaxies. We further use a parameter ξ to describe the number ratio of Compton-thick AGNs with $\log N_{\text{H}} = 24-25$ to those with $\log N_{\text{H}} = 23-24$. For the case of $\xi = 0.5$, our XRB synthesis calculation shows that the XRB contributed by active and inactive galaxies (type I/II Compton-thin AGNs + Compton-thick AGNs+RIAFs in inactive galaxies) can match the observed XRB for mass accretion rates $\dot{m}_{\text{inact}}^{\text{aver}} \simeq 2.0 \times 10^{-4}$ (see Fig. 7 for the case of $\rho_{\text{bh}}^{\text{local}} = 4.0 \times 10^5 M_{\odot} \text{Mpc}^{-3}$). A slightly higher accretion rate 2.5×10^{-4} is required for the case of $\rho_{\text{bh}}^{\text{local}} = 2.5 \times 10^5 M_{\odot} \text{Mpc}^{-3}$. If the contribution from the RIAFs in inactive galaxies is not considered, the same number of the Compton-thick AGNs with $\log N_{\text{H}} = 24-25$ as those with $\log N_{\text{H}} = 23-24$ is required to reproduce the observed XRB (see the yellow line in Fig. 7). In Fig. 8, we find that the contribution to the XRB from inactive galaxies can be neglected compared with that from Compton-thick AGNs, if $\dot{m}_{\text{inact}}^{\text{aver}} \lesssim 10^{-4}$. Corresponding to such constraints on the average accretion rates for inactive galaxies, we find that less than ~ 5 per cent, or even less than ~ 2 per cent if Compton-thick AGNs are considered, of the local massive black hole mass density was accreted during the radiatively inefficient accretion phases (see Table 1). The constraints of the XRB can only give upper limits on $\dot{m}_{\text{inact}}^{\text{aver}}$ for inactive galaxies, and we cannot rule out the possibility that inactive galaxies are accreting at rates significantly lower than 10^{-4} . This may be resolved by deep surveys on faint X-ray sources in hard X-ray bands, which is beyond the scope of this paper.

The detailed ADAF spectral calculations by Di Matteo et al. (1999) showed that many sources at redshift $z \sim 2-3$ with ADAFs accreting at the rates close to the critical value would be required to reproduce the observed spectral shape of the XRB with an energy peak at ~ 30 keV. However, Cao (2005)'s spectral calculations for RIAFs accreting at the critical value showed higher energy peaks at several hundred keV, which are unable to reproduce the observed spectral shape of the XRB (see Fig. 2 in Cao, 2005). The reason is that Cao (2005) adopted a larger δ than that used by Di Matteo et al. (1999) for traditional

ADAFs, which leads to higher electron temperatures of the accretion flows (see Cao 2005, for details). Di Matteo et al. (1999)'s calculations are limited to the spectral shape, which have not included the contribution of the ADAFs in all galaxies to the XRB quantitatively, and the contribution of normal bright AGNs has not been considered either. Our present calculations show that the spectra of the RIAFs surrounding Kerr black holes have peaks at around 10-100 keV, which depend sensitively on accretion rates (see Fig. 4). We find that our model calculations can fit both the intensity and the spectral shape of the XRB very well, if the RIAFs surrounding the Kerr black holes with $a \sim 0.9$ in inactive galaxies are accreting at $\dot{m}_{\text{inact}}^{\text{aver}} \simeq 1-3 \times 10^{-4}$. Cao (2005) calculated the contribution to the XRB from the RIAFs accreting at the critical rate, and found that the timescale for the sources accreting at the critical rate should be much shorter than the bright AGN lifetime. In that work, it was found that the spectral shape of the XRB cannot be reproduced even the RIAFs' contribution is included. Our present calculations imply the contribution from the RIAFs in the inactive galaxies accreting at $\simeq 1-3 \times 10^{-4}$ should dominate over that from those accreting at the critical value. It means that the timescale of AGNs accreting at around the critical value should be even shorter than that given by Cao (2005).

In this work, we have to assume the black holes in all inactive galaxies are accreting at an average rate $\dot{m}_{\text{inact}}^{\text{aver}}$, because we are almost ignorant of how the accretion rate evolves with time in active/inactive galaxies. A more realistic possibility may be that the massive black holes in inactive galaxies are accreting at different rates from far below $\sim 10^{-5}$ up to the critical value of ~ 0.01 , of which the stacked spectra (combined with the contribution from the type I/II AGNs) may reproduce the observed XRB. The spectrum of the RIAF accreting at the critical value is peaked at ~ 100 keV, due to the saturated Comptonization (see Fig. 1 in Cao 2005). These RIAFs are X-ray luminous, and therefore much more inactive galaxies accreting at very low rates ($\ll \dot{m}_{\text{inact}}^{\text{aver}}$) are required to reproduce the intensity of the XRB. However, the spectral shape of the XRB with an energy peak ~ 30 keV cannot be fitted in this way, because the energy peaks of the RIAF spectra are around several hundred keV while they are accreting at $\dot{m} \lesssim 10^{-4}$ (see Figs. 3 and 4). It means the contribution of the RIAFs accreting at around the critical value to the XRB should be unimportant compared with other inactive galaxies, which, again, suggests that the accretion rates of the RIAFs in inactive galaxies should decrease very rapidly after the accretion mode transition. It provides evidence of the feedback on the circumnuclear gases from the nuclear radiation, which is qualitatively consistent with the numerical simulations (see Fig. 2 in Di Matteo et al. 2005).

The RIAF may have winds, and a power-law radius-dependent accretion rate, $\dot{m}(r) \propto r^{-p_w}$ ($p_w > 0$), is assumed, though the detailed physics is still unclear (Blandford & Begelman 1999). As most X-ray emission is from the inner region of the accretion flow near the black hole, the X-ray spectrum of a RIAF is similar to a RIAF with winds, provided they have the same accretion rate at their inner edge. In this work, we are investigating the growth of black holes, so we focus on the accretion rate at the inner edge of the accretion flow. Thus, the conclusions will not be altered, even if winds are present in the RIAFs.

TABLE 1
THE SUMMARY OF DIFFERENT MODELS

Model	$\dot{m}_{\text{inact}}^{\text{aver}}$	ϵ	$\rho_{\text{bh}}^{\text{local}^a}$	$\rho_{\text{bh}}^{\text{B}}(0)/\rho_{\text{bh}}^{\text{local}}$	ϵ	$\rho_{\text{bh}}^{\text{local}^a}$	$\rho_{\text{bh}}^{\text{B}}(0)/\rho_{\text{bh}}^{\text{local}}$
A	1.0×10^{-3}	0.122	2.5×10^5	0.162	0.080	4.0×10^5	0.162
B	3.0×10^{-4}	0.110	2.5×10^5	0.051	0.071	4.0×10^5	0.051
C	2.0×10^{-4}	0.108	2.5×10^5	0.034	0.070	4.0×10^5	0.035
D	1.0×10^{-4}	0.106	2.5×10^5	0.017	0.069	4.0×10^5	0.017
E	0.0	0.105	2.5×10^5	0.0	0.068	4.0×10^5	0.0

^a in units of $M_{\odot} \text{Mpc}^{-3}$.

This work is supported by the National Science Fund for Distinguished Young Scholars (grant 10325314), and the

NSFC (grant 10333020).

REFERENCES

- Armitage P.J. 1998, *ApJ*, 501, L189
 Bisnovaty-Kogan G. S., & Lovelace R. V. E. 1997, *ApJ*, 486, L43
 Bisnovaty-Kogan G. S., Lovelace R. V. E., 2000, *ApJ*, 529, 978
 Blandford R. D., & Begelman M. C. 1999, *MNRAS*, 303, L1
 Boyle, B. J., Georgantopoulos, I., Blair, A. J., Stewart, G. C., Griffiths, R. E., Shanks, T., Gunn, K. F., & Almaini, O. 1998, *MNRAS*, 296, 1
 Boyle, B. J., Griffiths, R. E., Shanks, T., Stewart, G. C., & Georgantopoulos, I. 1993, *MNRAS*, 260, 49
 Cao, X. 2005, *ApJ*, 631, L101
 Comastri, A., Setti, G., Zamorani, G., & Hasinger, G. 1995, *A&A*, 296, 1
 Cowie, L. L., Barger, A. J., Bautz, M. W., Brandt, W. N., & Garmire, G. P. 2003, *ApJ*, 584, L57
 Di Matteo, T., Esin, A., Fabian, A. C., & Narayan, R. 1999, *MNRAS*, 305, L1
 Di Matteo, T., & Fabian, A. C. 1997, *MNRAS*, 286, 393
 Di Matteo, T., Springel, V., & Hernquist, L. 2005, *Nature*, 433, 604
 Elvis, M., Risaliti, G., & Zamorani, G. 2002, *ApJ*, 565, L75
 Ferrarese, L., & Merritt, D. 2000, *ApJ*, 539, L9
 Gebhardt, K. et al. 2000, *ApJ*, 539, L13
 Gilli, R., Risaliti, G., & Salvati, M. 1999, *A&A*, 347, 424
 Haehnelt, M. G., & Rees, M. J. 1993, *MNRAS*, 263, 168
 Haiman, Z., & Menou, K. 2000, *ApJ*, 531, 42
 Hasinger, G. 1998, *Astronomische Nachr.*, 319, 37
 Hawley, J.F., Gammie, C.F., & Balbus, S.A. 1996, *ApJ*, 464, 690
 Hawley, J.F., & Balbus, S.A. 2002, *ApJ*, 573, 738
 Hopkins, P. F., Hernquist, L., Cox, T. J., Di Matteo, T., Robertson, B., & Springel, V. 2005, *ApJ*, 632, 81
 Hopkins, P.F., Narayan, R., & Hernquist, L. 2006, *ApJ*, 643, 641
 Kauffmann, G., & Haehnelt, M. 2000, *MNRAS*, 311, 576
 Maccacaro, T., della Ceca, R., Gioia, I. M., Morris, S. L., Stocke, J. T., & Wolter, A. 1991, *ApJ*, 374, 117
 Madau, P., Ghisellini, G., & Fabian, A. C. 1994, *MNRAS*, 270, L17
 Manmoto, T. 2000, *ApJ*, 534, 734
 Marconi, A., Risaliti, G., Gilli, R., Hunt, L. K., Maiolino, R., & Salvati, M. 2004, *MNRAS*, 351, 169
 Matt, G., & Fabian, A. C. 1994, *MNRAS*, 267, 187
 McLure, R. J., & Dunlop, J. S. 2004, *MNRAS*, 352, 1390
 Miyaji, T., Hasinger, G., & Schmidt, M. 2000, *A&A*, 353, 25
 Narayan, R., 2002, in *Lighthouses of the Universe: The Most Luminous Celestial Objects and Their Use for Cosmology Proceedings of the MPA/ESO/*, p. 405
 Narayan, R., Mahadevan, R., & Quataert, E. 1998, in *Theory of Black Hole Accretion Disks*, edited by Marek A. Abramowicz, Gunnlaugur Bjornsson, and James E. Pringle.
 Narayan, R., & Yi, I. 1995, *ApJ*, 452, 710
 Nicastro, F., et al. 2000, *ApJ*, 536, 718
 Page, M. J., Mason, K. O., McHardy, I. M., Jones, L. R., & Carrera, F. J. 1997, *MNRAS*, 291, 324
 Salucci, P., Szuszkiewicz, E., Monaco, P., & Danese, L. 1999, *MNRAS*, 307, 637
 Schmidt, M., et al. 1998, *A&A*, 329, 495
 Sheth, R.K. et al. 2003, *ApJ*, 594, 225
 Soltan, A. 1982, *MNRAS*, 200, 115
 Tamura, N., Ohta, K., & Ueda, Y. 2006, *MNRAS*, 365, 134
 Ueda, Y., Akiyama, M., Ohta, K., & Miyaji, T. 2003, *ApJ*, 598, 886
 Wang, J.-M. et al. 2006, *ApJ*, 642, L111
 Wu, Q., & Cao, X. 2006, *PASP*, 118, 1098
 Wyithe, J. S. B., & Loeb, A. 2003, *ApJ*, 595, 614
 Yu, Q., & Tremaine, S. 2002, *MNRAS*, 335, 965